
ROBUST MULTIMODAL LEARNING WITH MISSING MODALITIES VIA PARAMETER-EFFICIENT ADAPTATION

Md Kaykobad Reza¹, Ashley Prater-Bennette², M. Salman Asif¹

¹ University of California Riverside, CA 92508, USA

² Air Force Research Laboratory, Rome, NY 13441, USA

mreza025@ucr.edu, ashley.prater-bennette@us.af.mil, sasif@ucr.edu

ABSTRACT

Multimodal learning seeks to utilize data from multiple sources to improve the overall performance of downstream tasks. It is desirable for redundancies in the data to make multimodal systems robust to missing or corrupted observations in some correlated modalities. However, we observe that the performance of several existing multimodal networks significantly deteriorates if one or multiple modalities are absent at test time. To enable robustness to missing modalities, we propose a simple and parameter-efficient adaptation procedure for pretrained multimodal networks. In particular, we exploit modulation of intermediate features to compensate for the missing modalities. We demonstrate that such adaptation can partially bridge performance drop due to missing modalities and outperform independent, dedicated networks trained for the available modality combinations in some cases. The proposed adaptation requires extremely small number of parameters (e.g., fewer than 0.7% of the total parameters) and applicable to a wide range of modality combinations and tasks. We conduct a series of experiments to highlight the missing modality robustness of our proposed method on 5 different datasets for multimodal semantic segmentation, multimodal material segmentation, and multimodal sentiment analysis tasks. Our proposed method demonstrates versatility across various tasks and datasets, and outperforms existing methods for robust multimodal learning with missing modalities.

1 Introduction

Multimodal learning (MML) [4, 63] is a general framework for processing, combining, and understanding information from multiple, diverse data sources. Fusing knowledge from multiple modalities (e.g., text, images, audio, and sensor data) is expected to provide more accurate and reliable systems. In recent years, MML has achieved remarkable success in a wide range of applications, including image segmentation [6, 55, 70], captioning [71, 65], classification [15, 46], sentiment analysis [50, 28], and autonomous driving [61, 45]. In all these applications, one often encounters situations where some modalities are corrupted or missing due to hardware limitations/failures, privacy concerns or data acquisition cost/constraints. The ability to handle corrupt or missing modalities is thus crucial for the robustness and reliability of multimodal systems. However, most of the existing multimodal models are not designed to handle corrupt or missing modalities. The primary focus of this paper is to study and enhance robustness of existing multimodal models in different missing modality scenarios.

Recent studies [38, 18, 41] have shown that MML is not inherently robust to missing modalities and performance can drop significantly when modalities are missing at test time. Existing approaches for robust MML usually work for specific combinations of modalities they are trained for and tend to perform poorly when applied to untrained combinations. For instance, one approach is to adopt robust training strategies such as modality dropout during training [42, 25], partial or full modality masking [2, 48], and knowledge distillation [52, 40]. These approaches either require specialized training strategies or utilize extra models/sub-networks to guide the underlying model. Another approach replaces uninformative tokens with aggregated informative tokens from different modalities or learns to predict tokens for the specific missing modalities [55, 58, 48]. Training such separate (independent) networks for every possible modality combination is not feasible specially when the number of input modalities is large. One recent approach for

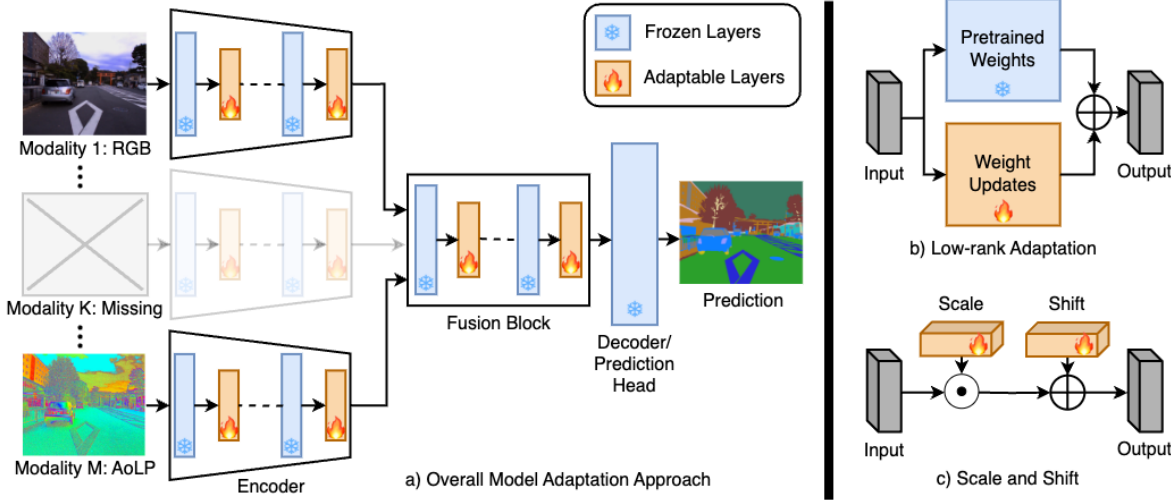


Figure 1: a) Overview of our approach for robust multimodal learning with missing modalities via parameter-efficient adaptation. A model pretrained on all the modalities is adapted using a small number of learnable parameters to handle different modality combinations. We insert adaptable layers after each layer of the encoders and the fusion block to learn the modulation as a function of the available input modalities to compensate for the missing modalities. The grayed-out branch (missing modality branch) is inactive and does not contribute to the output. b) Low-rank model adaption computes features using frozen weights and low-rank weight updates and combine them. c) Scale and shift feature adaptation transforms input by element-wise multiplication and addition. One set of parameters is learned for each modality combination.

robust MML is to impute missing modalities from the available modalities [64, 47, 11]. Performance of these methods depend on the generation model that imputes the missing modalities.

In this paper, we propose a parameter-efficient approach to adapt existing multimodal networks to perform well on different missing modality scenarios. **Our main objective is to modify the network in a controllable manner as a function of available modalities.** For instance, if a modality is missing, we seek to modify how the features from available modalities are extracted and fused for the inference. Instead of learning an independent network for each modality combination, our goal is to perform parameter-efficient adaptation. Figure 1 illustrates our proposed method, where a given multimodal network can be adapted to arbitrary modality combinations by transforming the intermediate features of the available input modalities at different layers. To achieve parameter-efficient adaptation, we propose to use simple linear transformations such as scaling and shifting to modulate the intermediate features or low-rank increments of features to compensate for the missing modalities. Our method does not require retraining the entire model or any specialized training strategy. The adapted networks provide significant performance improvement over the multimodal networks trained with all modalities and tested with missing modalities. Performance of the adapted models is also comparable or better than the models that are exclusively trained for each input modality combination. We present a series of experiments to evaluate our method and compare with existing methods for robust MML. We tested different parameter-efficient adaptation strategies and found intermediate feature modulation with scaling and shifting provides overall best performance with less than 0.7% of the total parameters.

Contributions. The main contributions can be summarized as follows.

- We propose parameter-efficient adaptation procedure for multimodal learning that is robust to missing modalities. The adapted model can easily switch to different network states based on the available modalities with minimal latency, computational, or memory overhead.
- The adapted networks provide notably improved performance with missing modalities when compared to models trained with all modalities and is comparable to or better than the networks trained for specific modality combinations.
- Our approach is versatile and adaptable to a wide range of multimodal tasks and models. Detailed evaluations on different datasets and tasks show that our approach outperforms existing baseline methods and robust models designed for specific tasks and datasets.

2 Related Work

Multimodal learning with missing modalities has been studied for different applications in recent years. For instance, robustness in vision-language tasks with multimodal transformers in [38], multimodal sentiment analysis in [41],

multimodal classification in [18], and multimodal action recognition in [58]. These studies have shown that the task performance can drop significantly when modalities are missing during test time.

Robust training strategies have been proposed to make models robust to different missing modalities. Such approaches include modality dropout during training [42, 25], unified representation learning [29], and supervised contrastive learning [14]. Modality masking during training has become a popular choice for enhancing robustness. [48] utilized complementary random masking, [21] used masked auto encoder, and [38] applied masked cross-modal attention for enhancing robustness of the underlying model. [18] proposed noisy perturbation of modalities during training for robust multimodal sentiment analysis. Recently, [30] proposed uni-modal ensemble with modality drop and substitution augmentation during training to adapt to different missing modality scenarios.

Design of robust models and fusion strategies is another approach for robust MML. [13] proposed a recursive meshing technique called SpiderMesh and [48] designed complementary random masking (CRM) and knowledge distillation based framework for robust RGB-thermal semantic segmentation. [55] proposed TokenFusion to dynamically detect and replace uninformative tokens with projected tokens from other modalities for robust RGB-depth semantic segmentation, image-to-image translation, and 3D object detection. [54] proposed a model that learns modality-shared and modality-specific features for robust brain tumour segmentation. [7] proposed a robust fusion strategy for multimodal classification. The main limitation of these methods is that they are generally designed for a specific modality combination and do not perform well when applied to other multimodal tasks [33].

Knowledge distillation and generation methods have also become popular for robust MML. Studies by [47] and [64] used GAN based generative models while [11] used VAE based generative models for imputing missing modalities from available input modalities for underlying multimodal tasks. Recently [44] introduced an approach to learn missing modality tokens from available modalities. Different knowledge distillation approaches have also been applied in several multimodal tasks. [52] proposed mean teacher and [40] introduced multimodal teacher for semi-supervised image segmentation. [48] and [18] applied self-distillation loss for robust RGB-thermal semantic segmentation. Apart from these approaches, weight space ensembling [59], policy learning [38] and optimal fusion strategy designing [40] were also studied for robust MML for various tasks.

These approaches are either designed for specific tasks/modality combinations [55, 48, 13] or require training extra modules/sub-networks [52, 40] for guiding the model under different missing modality scenarios. Our goal is to design a generic framework that is parameter-efficient and applicable to any model and modality combinations.

Parameter-efficient network adaptation has become very popular for uni-modal network adaptation in recent years [23, 34]. A number of parameter-efficient methods have been proposed for transfer learning [20, 10] and domain/task adaptation [24, 31]. We can divide the approaches into two major categories: low-rank/additive approach and feature transformation approach.

Low-rank/additive adaptation has been applied for uni-modal model fine-tuning and domain adaptation. For instance, LoRA [24], QLoRA [9], KronA [12] and KAdaptataion [22] learn low-rank factors for task/domain adaptation. Let W be the weight matrix of any dense layer of a given pretrained uni-modal model. These approaches learn a low-rank weight update matrix ΔW to transform the input x to that layer as $h = Wx + \Delta Wx$, where h is the updated feature. Since the update matrix ΔW is low-rank, the number of learnable parameters remains a fraction of the total number of model parameters. BitFit [5] is another approach that adapts the bias terms while keeping everything else frozen.

Feature modulation based approach is another parameter-efficient method to transform intermediate features of the pretrained model [26, 1, 60, 31]. As shown in Figure 1c, it applies a linear transformation to the given input token/feature with learnable scale (γ) and shift (β) parameters. Given an input token x , this approach generates the output token as $h = \gamma \odot x + \beta$, where γ, β, x, h are vectors of same dimension and \odot represents element-wise multiplication along the embedding dimension. These scale (γ) and shift (β) parameters are input-independent and learned during the training process to help the model adjust and fine-tune its representations for better performance on the underlying task.

Though parameter-efficient adaptation approaches have shown great potential in transfer learning, model fine tuning and task/domain adaptation, their potential remains unexplored in the context of missing modality in MML. In this study, we focus on parameter-efficient approaches to build our generic framework to enhance missing modality robustness in MML.

3 Proposed Method

In this section we first present a general framework for network adaptation for missing modalities. Then we discuss why we focus on parameter-efficient adaptation, present details of our proposed approach for missing modality adaptation and highlight the key benefits of our approach.

3.1 Network Adaptation for Missing Modalities

Let us denote the set of input modalities for a given multimodal task as $\mathcal{M} = \{m_1, \dots, m_M\}$. Given the full set \mathcal{M} , we can train a model f with parameters $\Theta_{\mathcal{M}}$ that maps inputs from all the modalities (denoted as $\mathcal{X}_{\mathcal{M}}$) to an output $y_{\mathcal{M}}$ as

$$y_{\mathcal{M}} = f(\mathcal{X}_{\mathcal{M}}; \Theta_{\mathcal{M}}). \quad (1)$$

While we can ensure the availability of all input modalities during training, it is possible that some modalities may be inaccessible at test time, especially after real-world deployment. Any subset of modalities \mathcal{M} can get missing due to hardware failure, data acquisition cost or privacy concerns. If we use a model trained on all the input modalities as denoted by (1), significant performance drop is observed when a subset of modalities gets missing during test time as shown in Table 1.

3.1.1 Naïve approach

When a subset of the modalities \mathcal{M} is missing, a simple and naïve approach is to train a new model for the available input modalities. Without loss of generality, suppose $\mathcal{K} \subset \mathcal{M}$ represents missing modalities. We can use the available input modalities $\mathcal{S} = \mathcal{M} \setminus \mathcal{K}$ to retrain the model f for a new set of parameters $\Theta_{\mathcal{S}}$ as

$$y_{\mathcal{S}} = f(\mathcal{X}_{\mathcal{S}}; \Theta_{\mathcal{S}}), \quad (2)$$

where $\mathcal{X}_{\mathcal{S}}$ represents input data for modalities in \mathcal{S} . In principle, we can train one model for every possible $\mathcal{S} \subset \mathcal{M}$ and use the corresponding model at the test time. Such an approach is infeasible because of computational and storage resources required to train models for a large number of possible modality combinations. Furthermore, deploying a large number of trained models and selecting one of them at test time is not feasible in real-world scenarios. Another drawback of this method is that, even though we would like $y_{\mathcal{S}} \approx y_{\mathcal{M}}$, the training process mentioned earlier does not guarantee it.

3.1.2 Parameter-efficient approach

We propose an alternative approach to adapt a single model for all subsets of input modalities $\mathcal{S} \subset \mathcal{M}$ in a parameter-efficient manner. First, we select a model f trained on the full set of modalities \mathcal{M} as shown in (1) and freeze the parameters $\Theta_{\mathcal{M}}$. Then we learn a small number of parameters $\Delta_{\mathcal{S}}$, specific to the available input modality set \mathcal{S} , and update the model as

$$\hat{y}_{\mathcal{S}} = f(\mathcal{X}_{\mathcal{S}}; \Theta_{\mathcal{M}}, \Delta_{\mathcal{S}}), \quad (3)$$

where $\hat{y}_{\mathcal{S}}$ represents the prediction of the updated model. Our goal is to keep $\hat{y}_{\mathcal{S}}$ close to all modality prediction $y_{\mathcal{M}}$ in the best case ($\hat{y}_{\mathcal{S}} \approx y_{\mathcal{M}}$) and close to the prediction $y_{\mathcal{S}}$ made by a model trained on the available input modalities in the worst case ($\hat{y}_{\mathcal{S}} \approx y_{\mathcal{S}}$).

The adaptation method shown in (3) is considered parameter-efficient if the number of parameters in $\Delta_{\mathcal{S}}$ is significantly smaller compared to the total number of parameters in $\Theta_{\mathcal{M}}$. During adaptation, we only train the learnable parameters $\Delta_{\mathcal{S}}$. In our experiments, as we discuss later, we keep $\Theta_{\mathcal{M}}$ frozen and demonstrate that less than 0.7% of the total parameters for $\Delta_{\mathcal{S}}$ are sufficient for network adaptation (see supplementary material for details).

3.1.3 Need for parameter-efficient adaptation

In the last few years, a number of approaches have been proposed for MML with missing modalities. To the best of our knowledge, parameter-efficient adaptation is still unexplored in this field. The current methods for robust MML, as discussed in Section 2, require retraining the whole model with specialized training strategy [48, 25] or utilize extra module/sub-network to guide the multi-modal model [40, 52]. Furthermore, these methods are not very generic and do not perform well on different missing modality scenarios as shown in Table 2 and 3. To solve these issues, we propose parameter-efficient adaptation for enhancing robustness of MML in the face of missing modalities. Our approach requires learning a very small number of parameters for different missing modality scenarios without the need to retrain the whole network. Furthermore, it is also applicable to diverse model architectures, tasks and modality combinations.

3.2 Parameter-Efficient Adaptation for Missing Modalities

In this section we first discuss how we adapt a given multimodal network for different missing modality scenarios. Then we discuss the reasons behind selecting intermediate feature modulation as the adaptation technique. Finally, we compare it with other parameter-efficient adaptation methods and discuss about some key benefits of our selected approach.

Adaptation for multimodal models. To the best of our knowledge, no parameter-efficient adaptation approach has been proposed or applied for multimodal model adaptation to handle missing modalities. We draw our motivation from low-rank adaptation and feature modulation based approach to compensate for the missing modalities. For instance, LoRA [24], BitFit [5], layer/feature normalization [1, 26], and scale and shift features (SSF) [31] approaches can enhance the representation capabilities of deep models for domain adaptation and model fine-tuning. We extend these adaptation approaches to build a generic framework that can transform the intermediate features of the available modalities to find an optimal feature representation to compensate for the performance gap due to missing modalities.

3.2.1 Training: model adaptation for missing modalities

Our approach for multi-modal model adaptation for missing modality is illustrated in Figure 1. Without loss of generality, let us assume a generic multi-modal model in which each modality goes through a separate modality-specific encoder. The extracted features from all the modalities are fused with a fusion block and the fused feature is passed to a decoder head for making prediction. Each encoder and the fusion block have multiple layers (linear/convolutional/norm layers). This setup can be easily generalized to models with shared encoder and/or different (early or mid) fusion strategy. We also do not make any assumption about the underlying model architecture.

We train this multimodal network f with all available modalities in \mathcal{M} to learn the parameters $\Theta_{\mathcal{M}}$ as shown in (1). Then we adapt f for different subsets of available modalities $\mathcal{S} \subset \mathcal{M}$. Unlike existing methods, we do not try to generate [39, 2], approximate [55, 54] or distill knowledge [48, 40] from any other modality/sub-network. Our goal is to learn a modified function for the available input modalities to appropriately learn and fuse features to compensate for any missing modality. Instead of re-training the entire network on the available modalities as shown in (2), we adapt the base network f and focus on learning a minimal set of parameters following (3).

To adapt the base model f , as shown in Figure 1a, we freeze the parameters $\Theta_{\mathcal{M}}$ (marked as  in light blue rectangles). This basically freezes all the layers in the model. To compensate for the missing modalities, we insert adaptable layers with learnable parameters $\Delta_{\mathcal{S}}$ (marked as  in light orange rectangles) after each frozen linear, convolutional, and norm (both batch norm and layer norm) layers. In cases where modalities are missing, we show the corresponding branch as grayed-out in Figure 1a indicating that they are inactive and do not contribute to the model output. Then we adapt f following (3) to learn the adaptable parameters $\Delta_{\mathcal{S}}$. While training the learnable parameters $\Delta_{\mathcal{S}}$ for a given modality combination, \mathcal{S} , we set the missing modalities to zero following standard practice [25, 40, 48, 33]. We minimized the cross-entropy loss with respect to $\Delta_{\mathcal{S}}$ for different modality combinations.

Below we discuss how to use low-rank and intermediate feature modulation-based multimodal network adaptation to accommodate missing modalities. We believe our framework is generic and can also incorporate other parameter-efficient adaptation approaches.

Low-rank/additive adaptation. We extend low-rank/additive approaches to adapt multimodal model for missing modalities. Let us assume that W_m be one of the weight matrices from any layer for the m^{th} input modality where $m \in \mathcal{S}$. As shown in Figure 1b, we learn a low-rank weight update matrix ΔW_m for that layer to transform the input $h_{m,i}$ to the layer as

$$h_{m,o} = W_m h_{m,i} + \Delta W_m h_{m,i}, \text{ for all } m \in \mathcal{S}, \quad (4)$$

where $h_{m,o}$ is the transformed output feature that is passed to the next layer in the model. Since the weight update matrix ΔW_m is low-rank, the total number of learnable parameters remains a fraction of the total number of model parameters. We can represent the learnable parameters $\Delta_{\mathcal{S}} = \{\Delta W_m\}_{m \in \mathcal{S}}$ as the collection of all low-rank update matrices.

Intermediate feature modulation. We extend SSF [31] method to work with multimodal models with missing modalities. The adaptable SSF layers modulate the intermediate tokens/features from each available modality at every layer as shown in Figure 1c. For the m^{th} input modality where $m \in \mathcal{S}$, we denote the learnable scale parameters as $\gamma_m \in \mathbb{R}^d$ and the learnable shift parameters as $\beta_m \in \mathbb{R}^d$ where d is the embedding dimension of the model. Since we insert SSF layers after each frozen layer in the pretrained model f , the output $h_{m,o} \in \mathbb{R}^{N \times d}$ from any frozen layer for the m^{th} input modality goes through the SSF layer that follows it. The SSF layer applies a linear transformation on $h_{m,o}$. We can formulate the linear transformation for multimodal input as follows:

$$h_{m,i} = \gamma_m \odot h_{m,o} + \beta_m, \text{ for all } m \in \mathcal{S}, \quad (5)$$

where $h_{m,i} \in \mathbb{R}^{N \times d}$ is the transformed feature which is fed to the next frozen layer in the model and N is the number of tokens. Note that if the output of any layer is of shape $(H \times W \times d)$ (for convolutional layers), we reshape it to $(N \times d)$, where $N = H \times W$, before applying the linear transformation. We reshape the transformed feature back to the original shape (if required) before passing it to the next layer. We can represent the learnable parameters as $\Delta_{\mathcal{S}} = \{\gamma_{\mathcal{S}}, \beta_{\mathcal{S}}\} = \{\gamma_m, \beta_m\}_{m \in \mathcal{S}}$. BitFit [5] method can also be used for adaptation as we only need to learn the

bias/shift terms β_m for all $m \in \mathcal{S}$. We modify (5) as

$$h_{m,i} = h_{m,o} + \beta_m, \text{ for all } m \in \mathcal{S}, \quad (6)$$

and the learnable parameters can be represented as $\Delta_{\mathcal{S}} = \{\beta_m\}_{m \in \mathcal{S}}$. Thus the intermediate features from each available modality are modulated to find a better representation to compensate for the missing modalities.

3.2.2 Inference: model adaptation for missing modalities

At the test time, we load the base multimodal model f with the pretrained weights $\Theta_{\mathcal{M}}$. If all the modalities are available, then we can use $\Theta_{\mathcal{M}}$ to make predictions. When a subset of the modalities are missing, we can select the learned parameters $\Delta_{\mathcal{S}}$ corresponding to the available input modalities \mathcal{S} , insert them into the model and use them to make prediction as follows:

$$\hat{y}_{\mathcal{S}} = \begin{cases} f(\mathcal{X}_{\mathcal{S}}; \Theta_{\mathcal{M}}) & \text{if } \mathcal{S} = \mathcal{M}, \\ f(\mathcal{X}_{\mathcal{S}}; \Theta_{\mathcal{M}}, \Delta_{\mathcal{S}}) & \text{if } \mathcal{S} \subset \mathcal{M}. \end{cases} \quad (7)$$

Since we are inserting the adaptable layers after each layer, it does not require any major change to the model architecture and can be done easily without reloading all the model parameters $\Theta_{\mathcal{M}}$. We just need to load the parameters in $\Delta_{\mathcal{S}}$ and insert them into the model. Since we only insert a very small number of additional parameters (less than 0.7% of the total model parameters), it adds very limited computational overhead. Furthermore, if a different subset of modalities becomes available, the adjustment is straightforward. We only need to replace the existing learned parameters $\Delta_{\mathcal{S}}$ with the corresponding parameters for the available modality set, ensuring adaptability and flexibility in handling diverse combinations of available modalities during the testing phase.

We only insert adaptable layers in the encoders and fusion blocks, while keeping the decoder/prediction head unchanged. We observed that using pretrained decoder/prediction head provided a good overall performance with several missing modalities.

3.2.3 Feature modulation vs low-rank adaptation

While we present three adaptation approaches in (4), (5), and (6), we select intermediate feature modulation with SSF (5) as the main approach for our experiments. We primarily selected this technique for robust MML with missing modalities because of its simplicity and effectiveness. Our experiments show that feature transformation via simple linear transformation with SSF works well for most of the scenarios compared to other parameter-efficient adaptation approaches as summarized in Table 4. We provided a detailed comparison in terms of mean accuracy, F1 score and % mIoU in Table 8, 9 and 10 in the supplementary section. SSF shows great promise in enhancing representation power [1], faster convergence [26], prevents loss of information in the representation learning process [60] and mitigates distribution mismatch between the upstream and downstream tasks [31]. These characteristics motivated us to extend this method for multimodal learning with missing modalities and build a generic framework that is very effective in learning the proper modulation of available input modalities to bridge the performance gap in the face of missing modalities.

Some key benefits of this approach are as follows. First, The parameters $\{\gamma, \beta\}$ are independent of the input features/modalities, which makes it applicable to diverse tasks and input modality combinations. Second, we can easily insert these learnable layers in existing models without changing the model architecture. We can easily switch/select the corresponding SSF parameters for a given input modality combination. Finally, it introduces extremely small number of additional learnable parameters. The resulting adaptation offers significant savings compared to training a separate model for each input combination or retraining the model using some specialized training strategy like modality dropout [25, 42] or knowledge distillation [48, 40].

4 Experiments and Results

We performed detailed experiments to evaluate the performance of our proposed method for multimodal semantic segmentation, multimodal material segmentation and multimodal sentiment analysis tasks on five datasets. We also present comparison with existing baseline methods that are robust to missing modalities.

4.1 Datasets

Multimodal semantic segmentation. We experimented on two datasets for multimodal semantic segmentation tasks: MFNet dataset [17] with RGB-Thermal input modalities and NYUDv2 dataset [49] with RGB-Depth input modalities.

Table 1: Performance of Pretrained, Dedicated, and Adapted networks with missing modalities. CMNeXt is the base model for multimodal semantic segmentation for MFNet and NYUDv2 datasets and multimodal material segmentation for MCubeS dataset. HHA-encoded images were used instead of raw depth maps. **Bold** letters represent best results.

Dataset	Input	Missing	Pretrained	Dedicated	Adapted (Ours)
MFNet	RGB-Thermal	-	60.10	60.10	-
	RGB	Thermal	53.71	55.86	55.22
	Thermal	RGB	35.48	53.34	50.89
NYUDv2	RGB-Depth	-	56.30	56.30	-
	RGB	Depth	51.19	52.18	52.82
	Depth	RGB	5.26	33.49	36.72
MCubeS	RGB-AoLP-DoLP-NIR	-	51.54	51.54	-
	RGB-AoLP-DoLP	NIR	49.06	49.48	51.11
	RGB-AoLP	DoLP-NIR	48.81	48.42	50.62
	RGB	AoLP-DoLP-NIR	42.32	48.16	50.43

These datasets are divided into train and test sets along with ground truth per-pixel annotation for the underlying semantic segmentation tasks.

Multimodal material segmentation. We used MCubeS dataset [32] for multimodal material segmentation having RGB, Angle of Linear Polarization (AoLP), Degree of Linear Polarization (DoLP) and Near-Infrared (NIR) images as input modalities. The dataset is divided into train, validation and test sets along with ground truth per-pixel annotation for 20 material classes.

Multimodal sentiment analysis. CMU-MOSI from [69] and CMU-MOSEI from [3] are two popular datasets for multimodal sentiment analysis using audio, visual and text as input modalities. They contain 2199 and 23453 annotated data samples, respectively, divided into train, validation, and test sets.

4.2 Implementation Details

To investigate missing modality adaptation performance in multimodal semantic and material segmentation tasks, we use the CMNeXt [70] as the base model. We use multimodal transformer [53] as the base model for multimodal sentiment analysis. We train the corresponding base model with all the input modalities for each dataset. To evaluate performance with missing modalities, we provide the available modalities and set the missing modalities to zero. To perform model adaptation for any modality subset $\mathcal{S} \subset \mathcal{M}$, we freeze the pretrained weights and insert learnable SSF layers. Then we fine tune the learnable parameters for 100 epochs for multimodal segmentation tasks and until convergence for multimodal sentiment analysis tasks.

For multimodal segmentation tasks, we set the initial learning rate to 6×10^{-5} and applied a polynomial learning rate scheduler with a power of 0.9. The first 10 epochs were set as the warm-up, during which the learning rate was set to 0.1 times the original rate. The scale parameters (γ) were initialized with all 1s and the shift parameters (β) were initialized with all 0s. We used cross-entropy loss function and AdamW optimizer as proposed in [37], with an epsilon value of 10^{-8} and a weight decay of 0.01. We used a batch size of 4 and report single scale performance for all the datasets. All other hyper-parameters and configurations are the same as [70]. For multimodal sentiment analysis tasks, we used the default settings for the datasets as configured in the codebase [66]. We have included additional details for each dataset and experimental setup in the supplementary section.

4.3 Baseline Methods

We report experiments and results for different methods that are listed as follows. **Pretrained** model refers to the base model that is trained with all the available modalities. We provide zeros for the missing modalities. **Modality Duplication** means that one of the available modalities is used as a substitution for the missing modality. **Dedicated** training refers to independent models trained for each input modality combination. **Adapted** model refers to the model that is adapted using our approach for each input modality combination.

Different robust methods have been proposed for different multimodal tasks. We compare our method with the following methods: masking and recursive meshing based approach SpiderMesh [13], variational probabilistic fusion based approach VPFNet [33], modality discrepancy reduction approach MDRNet [72], knowledge distillation and robust training based approach CRM [48] for robust RGB-thermal semantic segmentation. Dynamic channel exchange

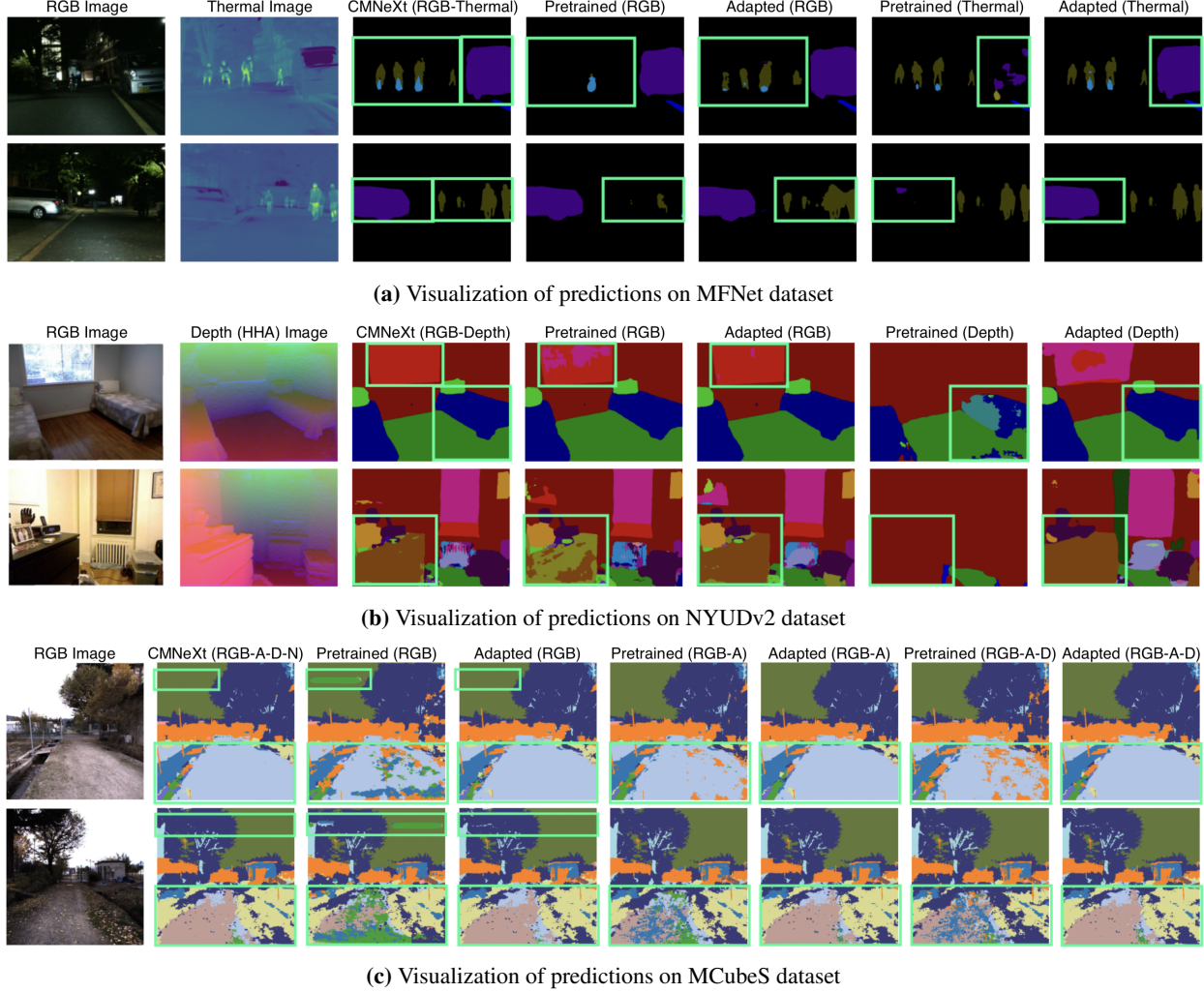


Figure 2: Examples of predicted segmentation maps for the Pretrained and Adapted models for multimodal semantic segmentation (on MFNet and NYUDv2) and material segmentation (on MCubeS). Title above each subimage shows method name (tested with available modalities). CMNeXt column shows the predictions with all the modalities. Segmentation quality improves significantly after model adaptation for all the input modality combinations. Green boxes highlight areas with salient differences in results (e.g., cars and humans missing in the Pretrained model with missing modalities but visible in the Adapted model). For MCubeS dataset, we only show RGB images and A, D and N denote angle of linear polarization, degree of linear polarization, and near-infrared, respectively.

based approach CEN [56], dynamic token selection/generation based approach TokenFusion [55], asymmetric fusion based approach AsymFusion [57] for robust RGB-depth semantic segmentation.

For every task/dataset, we adopted the experimental setup used in the corresponding previous studies. We used the reported results from prior works where possible. It is important to note that, because of this criteria, some of the baseline methods may only be present in specific experiments depending on the availability of their reported numbers. We also perform detailed comparison of SSF with other parameter-efficient adaptation techniques. For all the experiments we follow the same setup suggested by the corresponding papers and report mean accuracy (mAcc), F1 score and mean intersection over union (mIoU) when available.

Ablation studies and comparison of different parameter-efficient adaptation methods show that SSF-based adaptation provides overall best performance. We summarize the results for scale only, shift only, BitFit [5], norm layer fine-tuning and LoRA [24] in Table 4. We also add detailed comparison for all the datasets in the supplementary section of the paper.

Table 2: Performance comparison with existing robust methods for MFNet dataset. RGB and Thermal columns report performance when only RGB and Thermal are available. Average column reports average performance when one of the two modalities gets missing. ‘-’ indicates that results for those cells are not published. Mean accuracy (mAcc) and % mean intersection over union (mIoU) are shown for all the experiments.

Methods	RGB		Thermal		Average	
	mAcc	% mIoU	mAcc	% mIoU	mAcc	% mIoU
FuseNet [19]	11.11	10.31	41.33	36.85	26.22	23.58
MFNet [17]	26.62	24.78	19.65	16.64	23.14	20.71
RTFNet [51]	44.89	37.30	26.41	24.57	35.65	30.94
SAGate [6]	32.01	30.57	13.34	12.51	22.68	21.54
FEANet [8]	15.96	8.69	58.35	48.72	37.16	28.71
MDRNet [72]	57.11	45.89	41.98	30.19	49.55	38.04
VPFNet [33]	48.14	41.08	42.20	35.80	45.17	38.44
SpiderMesh [13]	-	39.60	-	50.50	-	45.05
CRM [48]	-	52.70	-	53.10	-	52.90
Adapted (Ours)	67.18	55.22	66.70	50.89	66.94	53.06

4.4 Experiments for Multimodal Segmentation

In this section, we present experiments for multimodal semantic segmentation on MFNet and NYUDv2 datasets, and multimodal material segmentation on MCubeS dataset. First, we show an overall comparison of our approach with existing baselines on Table 1 and then we compare our approach with existing robust methods on Table 2 and 3. We report the detailed results for multimodal material segmentation along with per class % intersection over union (IoU) comparisons between the Pretrained and Adapted models in the supplementary section of the paper.

4.4.1 Overall performance comparison

We present the performance comparison of Pretrained, Modality Duplication, Dedicated, and Adapted networks for different missing modalities in Table 1. We observe that the performance of the Pretrained model drops significantly with missing modalities. We see a 6.39% drop when Thermal is missing on MFNet dataset and 5.11% drop when Depth is missing on NYUDv2 dataset compared to the case when all modalities are available. The effect is amplified when RGB gets missing as we observe 24.62% drop on MFNet dataset and 51.04% drop on NYUDv2 dataset. On MCubeS dataset, we observe 2.48–9.22% drop in pretrained model when different modality combinations are missing. Similar trend of performance drop is observed for modality duplication approach though it performs better than pretrained models for most of the cases.

The overall performance of Adapted models with missing modalities is significantly better than Pretrained models and Modality Duplication approach. For MFNet, an improvement of 1.51% compared to the Pretrained model is observed when RGB is available and thermal is missing. The Adapted model performance is also close to the performance of Dedicated network trained for RGB only. The adapted model shows a significant improvement of 15.41% compared to the Pretrained model when RGB is missing. For NYUDv2 dataset, we see 1.63% and 31.46% performance improvement compared to Pretrained model when depth and RGB are missing, respectively. In both cases, the performance of the Adapted model is better than the Dedicated model. For all input combinations on MCubeS dataset, we see 1.82–8.11% performance improvement compared to the Pretrained model. The Adapted model performs better than Dedicated models in all the cases.

4.4.2 Performance comparison for RGB-Thermal semantic segmentation on MFNet dataset

We compare the performance of the Adapted model with existing robust models for RGB-thermal semantic segmentation on MFNet dataset in Table 2. The results show that the Adapted model offers the best average performance compared to the other baseline models, in terms of mean accuracy and % mIoU. Among the robust models, robust training and knowledge distillation based model CRM [48] shows competitive performance with the Adapted model. The Adapted model performs better when only RGB is available while CRM performs better when only Thermal is available. Notably CRM is designed specifically for RGB-Thermal pairs and requires specialized training approach and utilizes self-distillation loss between the clean and masked modalities to train the model. In contrast, our approach is applicable to any input modalities and does not require any specialized training technique. Our approach performs significantly better compared to masking and recursive meshing based SpiderMesh [13], variational probabilistic fusion based VPFNet [33] and modality discrepancy reduction based MDRNet [72] models.

Table 3: Performance comparison with existing robust methods for NYUDv2 dataset. RGB and Depth columns report performance when only RGB and Depth are available. Average column indicates average performance when one of the two modalities gets missing. * indicates that available codes and pretrained models from the authors were used to generate the results. Other results are from the corresponding papers.

Methods	RGB		Depth		Average	
	mAcc	% mIoU	mAcc	% mIoU	mAcc	% mIoU
FCN [36]	44.70	31.60	35.70	25.20	40.20	28.40
Dilated FCN-2s [27]	47.10	32.30	39.30	26.80	43.20	29.55
AsymFusion (R-101) [57]	59.00	46.50	45.60	34.30	52.30	40.40
CEN (R-101) [56] *	51.77	39.59	28.98	19.32	40.38	29.46
TokenFusion [55] *	63.49	49.32	46.83	36.84	55.16	43.08
Adapted (Ours)	67.96	52.82	52.42	36.72	60.19	44.77

Table 4: Performance comparison (% mIoU) of different parameter-efficient adaptation techniques for MFNet, NYUDv2, and MCubeS datasets. Each column reports mIoU of the Adapted model with the corresponding modalities, and Avg indicates average performance. A and D denote Angle and Degree of Linear Polarization.

Datasets	MFNet			NYUDv2			MCubeS			
	Methods	RGB	Thermal	Avg	RGB	Depth	Avg	RGB	RGB-A	RGB-A-D
Pretrained	53.71	35.48	44.60	51.19	5.26	28.23	42.32	48.81	49.06	46.73
Dedicated	55.86	53.34	54.60	52.18	33.49	42.84	48.16	48.42	49.48	48.69
Scale Only	54.77	49.23	52.00	53.04	36.12	44.58	50.16	50.55	51.13	50.61
Shift Only	54.57	48.96	51.77	53.04	36.25	44.65	50.13	50.40	50.86	50.46
BitFit	54.39	49.07	51.73	53.09	36.64	44.87	50.19	50.57	51.07	50.61
LoRA	54.19	47.45	50.82	52.87	34.97	43.92	49.59	50.07	50.80	50.15
Norm	54.65	47.49	51.07	53.05	34.73	43.49	49.95	50.51	51.07	50.51
Scale and Shift	55.22	50.89	53.06	52.82	36.72	44.77	50.43	50.62	51.11	50.72

4.4.3 Performance comparison for RGB-Depth semantic segmentation on NYUDv2 dataset

Table 3 shows the performance comparison with existing robust models for RGB-Depth semantic segmentation on NYUDv2 dataset. For our experiments, we use HHA-encoded images proposed by [16] instead of raw depth maps. On an average, the Adapted model performs better than the existing robust models. Dynamic token selection and substitution based model TokenFusion [55] performs slightly better (+0.12%) in terms of mIoU when Depth is available and RGB is missing, but shows larger drop (-5.59%) in mean accuracy. On the other hand, the Adapted model performs significantly better (+3.5% mIoU and +4.47% mean accuracy) when RGB is available and Depth is missing. The average performance of the Adapted model is also better than the TokenFusion model despite the fact that TokenFusion was designed to work with RGB-Depth pair, whereas the Adapted method is independent of input modalities. Our method also performs significantly better compared to dynamic channel exchange based CEN [56] and asymmetric fusion based AsymFusion [57] models.

4.4.4 Visualization of predictions

For qualitative analysis, we show some examples of the predicted segmentation maps from the Pretrained and Adapted models in Figure 2. For each dataset, we show the input images, predictions when all the modalities are available during both training and test time (CMNeXt column), predictions from the pretrained and adapted models for different available/missing modality scenarios (Available input modality names are shown in parentheses above each image). We see in Figure 2a, the Pretrained model fails to detect humans when only RGB images are available and cars when only Thermal images are available. The adapted model can detect both humans and cars with missing modalities.

For NYUDv2 dataset, as shown in Figure 2b, the Adapted model can detect window, bed, and furniture with higher accuracy than the Pretrained model with missing modalities. We only show the RGB input images for MCubeS dataset for brevity in Figure 2c. The Adapted model can identify sand, sky, and gravel with higher accuracy than the pretrained model. In all cases, the predictions from the Adapted model with missing modalities are closer to the predictions of the pretrained model with all the input modalities. We provide additional visualizations in the supplementary section of the paper.

Table 5: Comparison of our adaptation technique with existing methods for multimodal sentiment analysis.

Datasets	Methods	Audio		Visual		Audio-Visual		Average	
		ACC	F1	ACC	F1	ACC	F1	ACC	F1
CMU -MOSI	MuLT ([53])	48.31	40.98	52.44	51.77	48.93	41.95	49.89	44.90
	MFN ([68])	56.86	44.81	55.95	42.94	56.86	51.07	56.56	46.27
	TFN ([67])	42.23	25.07	42.38	25.40	42.23	25.07	42.28	25.18
	BERT_MAG ([43])	57.77	42.31	57.77	42.31	57.77	42.31	57.77	42.31
	LMF ([35])	42.23	25.07	43.14	27.54	43.29	27.61	42.89	26.74
	Adapted (Ours)	50.00	46.71	54.88	54.39	55.49	53.96	53.46	51.69
CMU - MOSEI	MuLT ([53])	37.15	20.12	38.28	23.70	41.91	32.78	39.11	25.53
	MFN ([68])	58.48	58.31	60.35	59.48	59.74	60.37	59.52	59.39
	TFN ([67])	37.15	20.12	37.15	20.12	37.15	20.12	37.15	20.12
	BERT_MAG ([43])	62.83	48.50	61.39	49.70	62.83	48.51	62.35	48.90
	LMF ([35])	42.38	34.48	57.15	57.85	55.94	56.63	51.82	49.65
	Adapted (Ours)	62.85	55.55	62.49	60.00	63.32	60.69	62.89	58.75

4.4.5 Performance comparison with parameter-efficient model adaption techniques

Apart from robust models, we also compare different parameter-efficient adaptation techniques. We summarize the results in Table 4. For MFNet dataset, SSF outperforms all the methods and performance is significantly better than the Pretrained model and close to the Dedicated models. For NYUDv2 and MCubeS datasets, the Adapted model performs better than both Pretrained and Dedicated models. These experiments also show that SSF performs better than other methods for most of the input modality combinations for all the datasets. We show a detailed comparison for each dataset in terms of mean accuracy, F1 score and % mIoU in the supplementary section of this paper.

4.5 Experiments for Multimodal Sentiment Analysis

We tested our adaptation method for multimodal sentiment analysis on CMU-MOSI [69] and CMU-MOSEI [3] datasets, and report the results in Table 5. We use multimodal transformer (MuLT) [53] as the base model and adapt it using our approach. We observed that when text is available and either audio or video or both are missing at the test time, the performance does not drop significantly. Similar trend was reported in [18]. If text is missing at test time, then the performance of the Pretrained model drops significantly. The Adapted models can partially compensate for missing text and offer significantly better performance compared to the pretrained model.

For CMU-MOSI dataset, we observe 1.69% and 2.44% improvement in accuracy over the Pretrained model performance when only audio and only visual are available, respectively. In all these scenarios, we also see larger improvement in F1 score. The adapted model offers significant improvement when audio-visual modalities are available and text is missing. It shows 6.56% improvement in terms of accuracy and 12.01% improvement in terms of F1 score over the Pretrained model. For CMU-MOSEI dataset, we see even greater improvement in all the metrics. Experiments show 25.7%, 24.21% and 21.41% improvement in accuracy for audio only, visual only and audio-visual scenarios compared to the Pretrained model. We also observe 27.91%-36.30% improvement in F1 score compared to the pretrained model.

We also compare our adaptation method with existing methods for multimodal sentiment analysis. The table shows that for CMU-MOSI dataset, BERT_MAG works better in terms of accuracy but our adaptation method works better in terms of F1 score. One thing to mention is that BERT_MAG uses a pretrained BERT model and finetunes it on the dataset but we are not using any pretraining on extra data. For CMU-MOSEI, our adaptation method works better for most of the cases. Which also demonstrates the generalizability and applicability of our approach to diverse modalities and different tasks.

5 Conclusion

Missing modalities at test time can cause significant degradation in the performance of multimodal systems. In this paper, we presented a simple and parameter-efficient adaptation method for robust multimodal learning with missing modalities. We demonstrated that simple linear operations can efficiently transform a single pretrained multimodal network and achieve performance comparable to multiple (independent) dedicated networks trained for different modality combinations. We evaluated the performance of our method and compared with existing robust methods for different multimodal segmentation and sentiment analysis tasks. Our method requires an extremely small number

of additional parameters (e.g., < 0.7% of the total parameters in most experiments), while significantly improving performance compared to existing baseline models and methods for different missing modality scenarios. Our adaptation strategy is applicable to different network architectures and tasks, which can be a versatile solution to build robust multimodal systems. In this work, our main focus was to enhance robustness of existing multimodal models and we did not try to optimize the number of parameters or find the optimal places to insert those learnable layers. Future study will explore these areas to further reduce the number of parameters and application of the approach beyond the tasks and datasets used in this study.

Reproducibility Statement

We are committed to ensuring the reproducibility of our research and to facilitate the broader scientific community in replicating and building upon our work. The source code and trained models are available at [github](https://github.com/CSIPlab/Robust-multimodal-learning)¹. We have provided a clear and comprehensive README.md file to guide users in setting up the environment, running the code, and reproducing the results in the paper. We outline the specific data preprocessing steps, list of hyperparameters and configurations used in our experiments in Section 4.2 in the main text and Section 2 in the supplementary section. We hope this makes it easy for others to replicate our experiments. We have provided scripts and instructions in our source code to reproduce the main experimental results presented in this paper. Additionally, we have provided pretrained models allowing others to directly reproduce the results.

Ethics Statement

To the best of our knowledge this work does not give rise to any significant ethical concerns.

Acknowledgements

This work is supported in part by AFOSR award FA9550-21-1-0330 and NSF CAREER award CCF-2046293.

References

- [1] Jimmy Lei Ba, Jamie Ryan Kiros, and Geoffrey E Hinton. Layer normalization. *Advances in Neural Information Processing Systems: Deep Learning Symposium. arXiv preprint arXiv:1607.06450*, 2016.
- [2] Roman Bachmann, David Mizrahi, Andrei Atanov, and Amir Zamir. MultiMAE: Multi-modal multi-task masked autoencoders. In *European Conference on Computer Vision*, 2022.
- [3] AmirAli Bagher Zadeh, Paul Pu Liang, Soujanya Poria, Erik Cambria, and Louis-Philippe Morency. Multimodal language analysis in the wild: CMU-MOSEI dataset and interpretable dynamic fusion graph. In *Proceedings of the 56th Annual Meeting of the Association for Computational Linguistics (Volume 1: Long Papers)*, pages 2236–2246, 2018.
- [4] Tadas Baltrušaitis, Chaitanya Ahuja, and Louis-Philippe Morency. Multimodal machine learning: A survey and taxonomy. *IEEE Transactions on Pattern Analysis and Machine Intelligence*, 41(2):423–443, 2018.
- [5] Elad Ben Zaken, Yoav Goldberg, and Shauli Ravfogel. BitFit: Simple parameter-efficient fine-tuning for transformer-based masked language-models. In *Proceedings of the 60th Annual Meeting of the Association for Computational Linguistics (Volume 2: Short Papers)*, pages 1–9, 2022.
- [6] Xiaokang Chen, Kwan-Yee Lin, Jingbo Wang, Wayne Wu, Chen Qian, Hongsheng Li, and Gang Zeng. Bi-directional cross-modality feature propagation with separation-and-aggregation gate for RGB-D semantic segmentation. In *European Conference on Computer Vision (ECCV)*, 2020.
- [7] Jun-Ho Choi and Jong-Seok Lee. EmbraceNet: A robust deep learning architecture for multimodal classification. *Information Fusion*, 51:259–270, 2019.
- [8] Fuqin Deng, Hua Feng, Mingjian Liang, Hongmin Wang, Yong Yang, Yuan Gao, Junfeng Chen, Junjie Hu, Xiyue Guo, and Tin Lun Lam. FEANet: Feature-enhanced attention network for RGB-thermal real-time semantic segmentation. In *2021 IEEE/RSJ International Conference on Intelligent Robots and Systems (IROS)*, pages 4467–4473. IEEE, 2021.

¹<https://github.com/CSIPlab/Robust-multimodal-learning>

[9] Tim Dettmers, Artidoro Pagnoni, Ari Holtzman, and Luke Zettlemoyer. Qlora: Efficient finetuning of quantized llms. *arXiv preprint arXiv:2305.14314*, 2023.

[10] Ning Ding, Yujia Qin, Guang Yang, Fuchao Wei, Zonghan Yang, Yusheng Su, Shengding Hu, Yulin Chen, Chi-Min Chan, Weize Chen, et al. Parameter-efficient fine-tuning of large-scale pre-trained language models. *Nature Machine Intelligence*, 5(3):220–235, 2023.

[11] Reuben Dorent, Samuel Joutard, Marc Modat, Sébastien Ourselin, and Tom Vercauteren. Hetero-modal variational encoder-decoder for joint modality completion and segmentation. In *Medical Image Computing and Computer Assisted Intervention–MICCAI 2019: 22nd International Conference, Shenzhen, China, October 13–17, 2019, Proceedings, Part II* 22, pages 74–82. Springer, 2019.

[12] Ali Edalati, Marzieh Tahaei, Ivan Kobyzev, Vahid Partovi Nia, James J. Clark, and Mehdi Rezagholizadeh. Krona: Parameter efficient tuning with kronecker adapter, 2022.

[13] Siqi Fan, Zhe Wang, Yan Wang, and Jingjing Liu. SpiderMesh: Spatial-aware demand-guided recursive meshing for RGB-T semantic segmentation. *arXiv:2303.08692*, 2023.

[14] Ahmed Gomaa, Andreas Maier, and Ronak Kosti. Supervised contrastive learning for robust and efficient multi-modal emotion and sentiment analysis. In *2022 26th International Conference on Pattern Recognition (ICPR)*, pages 2423–2429. IEEE, 2022.

[15] Matthieu Guillaumin, Jakob Verbeek, and Cordelia Schmid. Multimodal semi-supervised learning for image classification. In *2010 IEEE Computer Society Conference on Computer Vision and Pattern Recognition*, pages 902–909. IEEE, 2010.

[16] Saurabh Gupta, Ross Girshick, Pablo Arbeláez, and Jitendra Malik. Learning rich features from RGB-D images for object detection and segmentation. In *European Conference on Computer Vision*, pages 345–360, 2014.

[17] Qishen Ha, Kohei Watanabe, Takumi Karasawa, Yoshitaka Ushiku, and Tatsuya Harada. MFNet: Towards real-time semantic segmentation for autonomous vehicles with multi-spectral scenes. In *2017 IEEE/RSJ International Conference on Intelligent Robots and Systems (IROS)*, pages 5108–5115, 2017.

[18] Devamanyu Hazarika, Yingting Li, Bo Cheng, Shuai Zhao, Roger Zimmermann, and Soujanya Poria. Analyzing modality robustness in multimodal sentiment analysis. In *Proceedings of the 2022 Conference of the North American Chapter of the Association for Computational Linguistics: Human Language Technologies*, pages 685–696, Seattle, United States, July 2022. Association for Computational Linguistics.

[19] Caner Hazirbas, Lingni Ma, Csaba Domokos, and Daniel Cremers. FuseNet: Incorporating depth into semantic segmentation via fusion-based CNN architecture. In *Asian Conference on Computer Vision*, 2016.

[20] Junxian He, Chunting Zhou, Xuezhe Ma, Taylor Berg-Kirkpatrick, and Graham Neubig. Towards a unified view of parameter-efficient transfer learning. In *International Conference on Learning Representations*, 2022.

[21] Kaiming He, Xinlei Chen, Saining Xie, Yanghao Li, Piotr Dollár, and Ross Girshick. Masked autoencoders are scalable vision learners. In *Proceedings of the IEEE/CVF Conference on Computer Vision and Pattern Recognition*, pages 16000–16009, 2022.

[22] Xuehai He, Chunyuan Li, Pengchuan Zhang, Jianwei Yang, and Xin Eric Wang. Parameter-efficient model adaptation for vision transformers. *Proceedings of the AAAI Conference on Artificial Intelligence*, 37(1):817–825, Jun. 2023.

[23] Neil Houlsby, Andrei Giurgiu, Stanislaw Jastrzebski, Bruna Morrone, Quentin De Laroussilhe, Andrea Gesmundo, Mona Attariyan, and Sylvain Gelly. Parameter-efficient transfer learning for NLP. In Kamalika Chaudhuri and Ruslan Salakhutdinov, editors, *Proceedings of the 36th International Conference on Machine Learning*, volume 97 of *Proceedings of Machine Learning Research*, pages 2790–2799. PMLR, 09–15 Jun 2019.

[24] Edward J Hu, Yelong Shen, Phillip Wallis, Zeyuan Allen-Zhu, Yuanzhi Li, Shean Wang, Lu Wang, and Weizhu Chen. LoRA: Low-rank adaptation of large language models. In *International Conference on Learning Representations*, 2022.

[25] Ahmed Hussen Abdelaziz, Barry-John Theobald, Paul Dixon, Reinhard Knothe, Nicholas Apostoloff, and Sachin Kajareker. Modality dropout for improved performance-driven talking faces. In *Proceedings of the 2020 International Conference on Multimodal Interaction*, pages 378–386, 2020.

[26] Sergey Ioffe and Christian Szegedy. Batch normalization: Accelerating deep network training by reducing internal covariate shift. In *International Conference on Machine Learning*, pages 448–456, 2015.

[27] Sharif Amit Kamran and Ali Shihab Sabbir. Efficient yet deep convolutional neural networks for semantic segmentation. In *2018 International Symposium on Advanced Intelligent Informatics (SAIN)*, pages 123–130, 2018.

[28] Ramandeep Kaur and Sandeep Kautish. Multimodal sentiment analysis: A survey and comparison. *Research Anthology on Implementing Sentiment Analysis Across Multiple Disciplines*, pages 1846–1870, 2022.

[29] Kenneth Lau, Jonas Adler, and Jens Sjölund. A unified representation network for segmentation with missing modalities. *arXiv preprint arXiv:1908.06683*, 2019.

[30] Siting Li, Chenzhuang Du, Yue Zhao, Yu Huang, and Hang Zhao. What makes for robust multi-modal models in the face of missing modalities?, 2023.

[31] Dongze Lian, Daquan Zhou, Jiashi Feng, and Xinchao Wang. Scaling & shifting your features: A new baseline for efficient model tuning. In *Advances in Neural Information Processing Systems (NeurIPS)*, 2022.

[32] Yupeng Liang, Ryosuke Wakaki, Shohei Nobuhara, and Ko Nishino. Multimodal material segmentation. In *Proceedings of the IEEE/CVF Conference on Computer Vision and Pattern Recognition (CVPR)*, pages 19800–19808, June 2022.

[33] Baihong Lin, Zengrong Lin, Yulan Guo, Yulan Zhang, Jianxiao Zou, and Shicai Fan. Variational probabilistic fusion network for RGB-T semantic segmentation. *arXiv preprint arXiv:2307.08536*, 2023.

[34] Haokun Liu, Derek Tam, Mohammed Muqeeth, Jay Mohta, Tenghao Huang, Mohit Bansal, and Colin A Raffel. Few-shot parameter-efficient fine-tuning is better and cheaper than in-context learning. In S. Koyejo, S. Mohamed, A. Agarwal, D. Belgrave, K. Cho, and A. Oh, editors, *Advances in Neural Information Processing Systems*, volume 35, pages 1950–1965. Curran Associates, Inc., 2022.

[35] Zhun Liu, Ying Shen, Varun Bharadhwaj Lakshminarasimhan, Paul Pu Liang, Amir Zadeh, and Louis-Philippe Morency. Efficient low-rank multimodal fusion with modality-specific factors. In *Annual Meeting of the Association for Computational Linguistics*, 2018.

[36] Jonathan Long, Evan Shelhamer, and Trevor Darrell. Fully convolutional networks for semantic segmentation. In *2015 IEEE Conference on Computer Vision and Pattern Recognition (CVPR)*, pages 3431–3440, 2015.

[37] Ilya Loshchilov and Frank Hutter. Decoupled weight decay regularization. In *International Conference on Learning Representations*, 2019.

[38] Mengmeng Ma, Jian Ren, Long Zhao, Davide Testuggine, and Xi Peng. Are multimodal transformers robust to missing modality? In *Proceedings of the IEEE/CVF Conference on Computer Vision and Pattern Recognition*, pages 18177–18186, 2022.

[39] Mengmeng Ma, Jian Ren, Long Zhao, Sergey Tulyakov, Cathy Wu, and Xi Peng. Smil: Multimodal learning with severely missing modality. In *Proceedings of the AAAI Conference on Artificial Intelligence*, volume 35, pages 2302–2310, 2021.

[40] Harsh Maheshwari, Yen-Cheng Liu, and Zsolt Kira. Missing modality robustness in semi-supervised multi-modal semantic segmentation. *arXiv preprint arXiv:2304.10756*, 2023.

[41] Brandon McKinzie, Joseph Cheng, Vaishaal Shankar, Yinfei Yang, Jonathon Shlens, and Alexander Toshev. On robustness in multimodal learning. *arXiv preprint arXiv:2304.04385*, 2023.

[42] Natalia Neverova, Christian Wolf, Graham Taylor, and Florian Nebout. ModDrop: Adaptive multi-modal gesture recognition. *IEEE Transactions on Pattern Analysis and Machine Intelligence*, 38(8):1692–1706, 2015.

[43] Wasifur Rahman, Md Kamrul Hasan, Sangwu Lee, AmirAli Bagher Zadeh, Chengfeng Mao, Louis-Philippe Morency, and Ehsan Hoque. Integrating multimodal information in large pretrained transformers. In Dan Jurafsky, Joyce Chai, Natalie Schluter, and Joel Tetreault, editors, *Proceedings of the 58th Annual Meeting of the Association for Computational Linguistics*, pages 2359–2369, Online, July 2020. Association for Computational Linguistics.

[44] Merey Ramazanova, Alejandro Pardo, Humam Alwassel, and Bernard Ghanem. Exploring missing modality in multimodal egocentric datasets, 2024.

[45] Giulia Rizzoli, Francesco Barbato, and Pietro Zanuttigh. Multimodal semantic segmentation in autonomous driving: A review of current approaches and future perspectives. *Technologies*, 10(4):90, 2022.

[46] Swalpa Kumar Roy, Ankur Deria, Danfeng Hong, Behnood Rasti, Antonio Plaza, and Jocelyn Chanussot. Multimodal fusion transformer for remote sensing image classification. *IEEE Transactions on Geoscience and Remote Sensing*, 2023.

[47] Anmol Sharma and Ghassan Hamarneh. Missing MRI pulse sequence synthesis using multi-modal generative adversarial network. *IEEE Transactions on Medical Imaging*, 39(4):1170–1183, 2019.

[48] Ukcheol Shin, Kyunghyun Lee, and In So Kweon. Complementary random masking for RGB-Thermal semantic segmentation. *arXiv preprint arXiv:2303.17386*, 2023.

[49] Nathan Silberman, Derek Hoiem, Pushmeet Kohli, and Rob Fergus. Indoor segmentation and support inference from RGBD images. In *European Conference on Computer Vision*, 2012.

[50] Mohammad Soleymani, David Garcia, Brendan Jou, Björn Schuller, Shih-Fu Chang, and Maja Pantic. A survey of multimodal sentiment analysis. *Image and Vision Computing*, 65:3–14, 2017.

[51] Yuxiang Sun, Weixun Zuo, and Ming Liu. RTFNet: RGB-Thermal Fusion Network for Semantic Segmentation of Urban Scenes. *IEEE Robotics and Automation Letters*, 4(3):2576–2583, July 2019.

[52] Antti Tarvainen and Harri Valpola. Mean teachers are better role models: Weight-averaged consistency targets improve semi-supervised deep learning results. *Advances in Neural Information Processing Systems*, 30, 2017.

[53] Yao-Hung Hubert Tsai, Shaojie Bai, Paul Pu Liang, J. Zico Kolter, Louis-Philippe Morency, and Ruslan Salakhutdinov. Multimodal transformer for unaligned multimodal language sequences. In *Proceedings of the 57th Annual Meeting of the Association for Computational Linguistics*, pages 6558–6569, Florence, Italy, July 2019. Association for Computational Linguistics.

[54] Hu Wang, Yuanhong Chen, Congbo Ma, Jodie Avery, Louise Hull, and Gustavo Carneiro. Multi-modal learning with missing modality via shared-specific feature modelling. In *Proceedings of the IEEE/CVF Conference on Computer Vision and Pattern Recognition*, pages 15878–15887, 2023.

[55] Yikai Wang, Xinghao Chen, Lele Cao, Wenbing Huang, Fuchun Sun, and Yunhe Wang. Multimodal token fusion for vision transformers. In *IEEE Conference on Computer Vision and Pattern Recognition (CVPR)*, 2022.

[56] Yikai Wang, Wenbing Huang, Fuchun Sun, Tingyang Xu, Yu Rong, and Junzhou Huang. Deep multimodal fusion by channel exchanging. In *Advances in Neural Information Processing Systems (NeurIPS)*, 2020.

[57] Yikai Wang, Fuchun Sun, Ming Lu, and Anbang Yao. Learning deep multimodal feature representation with asymmetric multi-layer fusion. In *ACM International Conference on Multimedia (ACM MM)*, 2020.

[58] Sangmin Woo, Sumin Lee, Yeonju Park, Muhammad Adi Nugroho, and Changick Kim. Towards good practices for missing modality robust action recognition. In *Proceedings of the AAAI Conference on Artificial Intelligence*, volume 37, 2023.

[59] Mitchell Wortsman, Gabriel Ilharco, Jong Wook Kim, Mike Li, Simon Kornblith, Rebecca Roelofs, Raphael Goncalves Lopes, Hannaneh Hajishirzi, Ali Farhadi, and Hongseok Namkoong. Robust fine-tuning of zero-shot models. In *Proceedings of the IEEE/CVF Conference on Computer Vision and Pattern Recognition*, pages 7959–7971, 2022.

[60] Yuxin Wu and Kaiming He. Group normalization, 2018.

[61] Yi Xiao, Felipe Codevilla, Akhil Gurram, Onay Urfalioglu, and Antonio M López. Multimodal end-to-end autonomous driving. *IEEE Transactions on Intelligent Transportation Systems*, 23(1):537–547, 2020.

[62] Enze Xie, Wenhui Wang, Zhiding Yu, Anima Anandkumar, Jose M Alvarez, and Ping Luo. SegFormer: Simple and efficient design for semantic segmentation with transformers. In *Neural Information Processing Systems (NeurIPS)*, 2021.

[63] Peng Xu, Xiatian Zhu, and David A Clifton. Multimodal learning with transformers: A survey. *IEEE Transactions on Pattern Analysis and Machine Intelligence*, 2023.

[64] Biting Yu, Luping Zhou, Lei Wang, Jurgen Fripp, and Pierrick Bourgeat. 3D cGAN based cross-modality MR image synthesis for brain tumor segmentation. In *2018 IEEE 15th International Symposium on Biomedical Imaging (ISBI 2018)*, pages 626–630. IEEE, 2018.

[65] Jun Yu, Jing Li, Zhou Yu, and Qingming Huang. Multimodal transformer with multi-view visual representation for image captioning. *IEEE Transactions on Circuits and Systems for Video Technology*, 30(12):4467–4480, 2019.

[66] Wenmeng Yu, Hua Xu, Ziqi Yuan, and Jiele Wu. Learning modality-specific representations with self-supervised multi-task learning for multimodal sentiment analysis. In *Proceedings of the AAAI Conference on Artificial Intelligence*, volume 35, pages 10790–10797, 2021.

[67] Amir Zadeh, Minghai Chen, Soujanya Poria, Erik Cambria, and Louis-Philippe Morency. Tensor fusion network for multimodal sentiment analysis. In Martha Palmer, Rebecca Hwa, and Sebastian Riedel, editors, *Proceedings of the 2017 Conference on Empirical Methods in Natural Language Processing*, pages 1103–1114, Copenhagen, Denmark, September 2017. Association for Computational Linguistics.

[68] Amir Zadeh, Paul Pu Liang, Navonil Mazumder, Soujanya Poria, Erik Cambria, and Louis-Philippe Morency. Memory fusion network for multi-view sequential learning. In *Proceedings of the Thirty-Second AAAI Conference on Artificial Intelligence and Thirtieth Innovative Applications of Artificial Intelligence Conference and Eighth AAAI Symposium on Educational Advances in Artificial Intelligence*, AAAI’18/IAAI’18/EAAI’18. AAAI Press, 2018.

- [69] Amir Zadeh, Rowan Zellers, Eli Pincus, and Louis-Philippe Morency. Multimodal sentiment intensity analysis in videos: Facial gestures and verbal messages. *IEEE Intelligent Systems*, 31(6):82–88, 2016.
- [70] Jiaming Zhang, Ruiping Liu, Hao Shi, Kailun Yang, Simon Reiß, Kunyu Peng, Haodong Fu, Kaiwei Wang, and Rainer Stiefelhagen. Delivering arbitrary-modal semantic segmentation. In *Proceedings of the IEEE/CVF Conference on Computer Vision and Pattern Recognition*, pages 1136–1147, 2023.
- [71] Dexin Zhao, Zhi Chang, and Shutao Guo. A multimodal fusion approach for image captioning. *Neurocomputing*, 329:476–485, 2019.
- [72] Shenlu Zhao, Yichen Liu, Qiang Jiao, Qiang Zhang, and Jungong Han. Mitigating modality discrepancies for RGB-T semantic segmentation. *IEEE Transactions on Neural Networks and Learning Systems*, pages 1–15, 2023.

SUPPLEMENTARY MATERIAL

1 Datasets

MFNet Dataset introduced by [17], is a popular dataset for RGB-thermal urban scene segmentation, particularly in the context of supporting autonomous driving applications. It comprises a total of 1569 aligned pairs of RGB-thermal images. Within this collection, 820 image pairs were captured during daytime, while 749 pairs were acquired during nighttime. The dataset is divided into distinct training and test sets, each accompanied by pixel-level annotations that define semantic labels for nine classes. Each image is 640×480 pixels.

NYU Depth v2 (NYUDv2) Dataset from [49] is a well-known dataset for RGB-D semantic segmentation. This dataset contains 1449 pairs of aligned RGB-depth images of indoor scenes. The images are divided into training and test sets containing 795 and 654 pairs of images respectively. The dataset also provides per pixel annotations for 13 classes, 40 classes and 894 classes ground truth semantic labels. For our experiments we used the standard 40 classes annotation. Each image is 640×480 pixels and the dataset contains both raw and processed depth maps. For our experiments we used HHA images as proposed by [16] instead of depth maps.

Multimodal Material Segmentation (MCubeS) Dataset was introduced by [32] for accurate multimodal material segmentation with the help of thermal and polarized images alongside RGB images. This dataset has four modalities: RGB, Angle of Linear Polarization, Degree of Linear Polarization and Near-Infrared. Alongside these modalities, the dataset also provides ground truth annotation for semantic and material segmentation. There are 500 image sets divided into train, validation and test sets having 302, 96 and 102 image sets respectively. The images are 1224×1024 pixels each and have 20 classes in total.

CMU-MOSI dataset from [69] is a popularly used for multimodal sentiment analysis. The dataset has 2199 samples each having audio, visual and text as input modalities. It is divided into train, validation and test sets containing 1284, 229 and 686 samples respectively along with annotated sentiment for each sample.

Table 6: Hyperparameters for the experiments on CMU-MOSI and CMU-MOSEI datasets for multimodal sentiment analysis.

Hyperparameters	CMU-MOSI	CMU-MOSEI
Batch Size	16	4
Initial Learning Rate	0.002	0.0005
Optimizer	Adam	Adam
Attention Dropout	0.3	0.4
Embedding Dropout	0.2	0.0
Output Dropout	0.5	0.5
Gradient Clip	0.6	0.6
Weight Decay	0.005	0.001
Temporal Conv Kernel Size (T/A/V)	5/5/5	5/1/3
# of Crossmodal Blocks	4	4

CMU-MOSEI is a large scale sentiment analysis dataset from [3]. It is 10 times larger than CMU-MOSI and contains audio, visual and text modalities along with ground truth sentiment annotations. The dataset contains 23453 samples divided into train, validation and test sets for multimodal sentiment analysis and emotion recognition.

2 Implementation Details

We used Python² 3.8.12 and PyTorch³ 1.9.0 to for our implementation. The experiments were done using two NVIDIA RTX 2080 Ti GPUs. We applied automatic mixed precision (AMP) training provided by PyTorch. For CMNeXt model, we use their publicly available code⁴ and models trained on all the available modalities for each dataset. We trained the multimodal transformer models on all the modalities using the available code and preprocessed data from the repository⁵ for CMU-MOSI and CMU-MOSEI datasets.

²<https://www.python.org/>

³<https://pytorch.org/>

⁴<https://github.com/jamycheung/DELIVER>

⁵<https://github.com/thuiar/MMSA>

Table 7: Learnable parameter counts for different parameter efficient model adaptation methods. As seen from the table, scale and shift introduce less than 0.7% of the total model parameters.

Method	Total Parameters (M)	Learnable Parameters (M)	% of Total Parameters
Norm	116.560	0.126	0.108
BitFit	116.560	0.378	0.324
LoRA	116.957	0.397	0.340
Scale and Shift	117.349	0.789	0.673

Table 8: Performance comparison with parameter efficient model adaptation techniques on CMNeXt model for MFNet dataset. Average column indicates average performance when one of the two modalities gets missing. Mean accuracy, F1 score and % mIoU are shown for all the experiments.

Methods	RGB			Thermal			Average		
	mAcc	F1	% mIoU	mAcc	F1	% mIoU	mAcc	F1	% mIoU
Pretrained	60.74	66.91	53.71	38.18	45.11	35.48	49.46	56.01	44.60
Dedicated	66.28	68.22	55.86	68.35	65.29	53.34	67.32	66.76	54.60
Scale Only	67.09	68.03	54.77	64.00	60.92	49.23	65.55	64.48	52.00
Shift Only	65.82	67.42	54.57	59.77	60.54	48.96	62.80	63.98	51.77
BitFit	66.49	67.40	54.39	61.06	60.59	49.07	63.78	64.00	51.73
LoRA	66.44	67.32	54.19	57.10	59.04	47.45	61.77	63.18	50.82
Norm	66.43	67.07	54.65	57.55	59.22	47.49	61.99	63.15	51.07
Scale and Shift	67.18	68.04	55.22	66.70	62.64	50.89	66.94	65.34	53.06

MFNet Dataset: We divided the 4 channel RGB-T images into three channel RGB and one channel thermal images. Then data pre-processing and augmentation was applied following CMNeXt from [70]. MiT-B4 from [62] was the backbone for the base CMNeXt model. One set of scale and shift parameters was learnt for each input modality combination. Input images were sized at 640×480 for both training and testing and we report single scale performance for all the experiments. The scale and shift parameters were trained for 100 epochs with a batch size of 4.

NYUDv2 Dataset: For processing depth maps, we follow SA-Gate by [6] and CMNeXt by [70] and use HHA-encoded images instead of raw depth maps. The already preprocessed dataset can be downloaded from the SA-Gate repository⁶. RGB and HHA images were sized at 640×480 pixels each and we used this size for training and testing. The backbone was set to MiT-B4 as suggested in CMNeXt paper. One set of scale and shift parameters was learnt for each input modality combination by feeding available input modalities and setting the missing modality to zero. We train the scale and shift parameters for 100 epochs with a batch size of 4 and report single scale performance.

MCubeS Dataset: We follow the same data pre-processing and augmentations used by the base CMNeXt model from [70]. MiT-B2 from [62] was used as the backbone for this dataset. We set the input image resolution to 512×512 during training and 1024×1024 during testing and report single scale performance with predicted segmentation maps sized at 1024×1024 . Similar to other two datasets, we train the learnable parameters for 100 epochs with a batch size of 4.

CMU-MOSI and CMU-MOSEI Datasets: We used Multimodal Transformer (MuLT) from [53] as the base model. Preprocessed datasets and all the configurations are available on the repository⁷. First we trained the multimodal transformer (MuLT) model on all the available modalities and then adapted the pretrained model for different missing modality scenarios. The hyperparameters for the experiments are shown in Table 6.

3 Number of Learnable Parameters

We report the number of learnable parameters for different parameter-efficient adaptation techniques (for multimodal segmentation) in Table 7. We insert scale and shift layers after each linear, convolutional and norm (both batch norm and layer norm) layers. The number of learnable parameter varies with the size of the backbone. We used MiT-B4 as the backbone while counting these learnable parameters. Scale and shift adds only 0.789M learnable parameters which

⁶https://github.com/charlesCCKX/RGBD_Semantic_Segmentation_PyTorch

⁷<https://github.com/thuiar/MMSA>

Table 9: Performance comparison with parameter efficient model adaptation techniques on CMNeXt model for NYUDv2 dataset. Average column indicates average performance when one of the two modalities gets missing. Mean accuracy, F1 score and % mIoU are shown for all the experiments.

Methods	RGB			Depth			Average		
	mAcc	F1	% mIoU	mAcc	F1	% mIoU	mAcc	F1	% mIoU
Pretrained	64.10	65.70	51.19	8.30	7.95	5.26	36.20	36.83	28.23
Dedicated	66.00	66.62	52.18	44.80	46.79	33.49	55.40	56.71	42.84
Scale Only	68.18	67.38	53.04	51.54	49.88	36.12	59.86	58.63	44.58
Shift Only	67.54	67.35	53.04	50.30	49.76	36.25	58.92	58.56	44.65
BitFit	67.31	67.33	53.09	50.68	50.27	36.64	59.00	58.80	44.87
LoRA	66.67	67.14	52.87	49.34	48.66	34.97	58.01	57.90	43.92
Norm	67.18	67.34	53.05	48.74	48.06	34.73	57.96	57.70	43.89
Scale and Shift	67.96	67.18	52.82	52.42	50.60	36.72	60.19	58.89	44.77

Table 10: Performance comparison with different parameter efficient model adaptation techniques on CMNeXt model for MCubeS dataset. Average column indicates the average performance. Mean accuracy, F1 score and % mIoU are shown for all the experiments.

Methods	RGB			RGB-AoLP			RGB-AoLP-DoLP			Average		
	mAcc	F1	% mIoU	mAcc	F1	% mIoU	mAcc	F1	% mIoU	mAcc	F1	% mIoU
Pretrained	51.63	55.91	42.32	58.66	62.00	48.81	60.06	62.43	49.06	56.78	60.11	46.73
Dedicated	57.70	60.95	48.16	57.56	61.17	48.42	59.12	61.91	49.48	58.13	61.34	48.69
Scale Only	59.64	63.06	50.16	60.28	63.55	50.55	60.96	64.14	51.13	60.29	63.58	50.61
Shift Only	59.82	63.17	50.13	60.10	63.36	50.40	60.61	63.78	50.86	60.18	63.44	50.46
BitFit	59.98	63.24	50.19	60.12	63.52	50.57	60.84	64.03	51.07	60.31	63.60	50.61
LoRA	59.08	62.50	49.59	59.81	63.05	50.07	60.69	63.84	50.80	59.86	63.13	50.15
Norm	59.57	62.89	49.95	60.22	63.49	50.51	60.98	64.08	51.07	60.26	63.49	50.51
Scale and Shift	60.23	63.41	50.43	60.40	63.59	50.62	60.94	64.04	51.11	60.52	63.68	50.72

is less than 0.7% of the total model parameters. Despite this very few parameters, it improves performance significantly in different missing modality scenarios. For this study we mainly focused on improving missing modality robustness and did not try to optimize the number of learnable parameters. We will leave that part for future studies.

4 Performance Comparison with Parameter Efficient Model Adaption Techniques

We performed a detailed performance comparison with other parameter efficient methods for the three segmentation datasets. The results are summarized in Table 8 for RGB-thermal segmentation on MFNet dataset, Table 9 for RGB-depth segmentation on NYUDv2 dataset and Table 10 for multimodal material segmentation on MCubeS dataset. For each method, we take a model trained on all the available modalities. Then we freeze the pretrained weights and tune the learnable parameters for the corresponding adaption method. We have shown mean accuracy, F1 score and % mIoU for each experiment.

4.1 Performance Comparison for RGB-Thermal Semantic Segmentation on MFNet Dataset

Table 8 summarizes the results on MFNet dataset when the base CMNeXt model is adapted with other parameter efficient model adaptation techniques. Experiments show that scale and shift shows the best performance in all three matrices compared to all other methods. It shows a significant improvement of +8.46% in mIoU, +9.33% in F1 score and +17.48% in mean accuracy on an average over the pretrained model. The average performance is also close to dedicatedly trained models.

4.2 Performance Comparison for RGB-Depth Semantic Segmentation on NYUDv2 Dataset

Similar trend is observed for RGB-Depth semantic segmentation on NYUDv2 dataset as shown in Table 9. Scale only and BitFit adapted models show slightly better performance for some of the matrices. But in most of the cases scale and shift adapted model performs better. For all the matrices, scale and shift shows a significant improvement of +16.54%

Table 11: Per class % IoU comparison between pretrained and adapted CMNeXt model on MFNet and MCubeS datasets. Adapted model show better performance for most of the classes leading to overall performance improvement. Here A, D and N stand for Angle of Linear Polarization (AoLP), Degree of Linear Polarization (DoLP) and Near-Infrared (NIR) respectively.

(a) Per class % IoU of pretrained and adapted CMNeXt model on MFNet dataset.

Modalities	Methods	Unlabeled	Car		Person		Bike		Curve		Car_Stop		Guardrail		Color_Cone		Bump		Mean
			Car	Person	Bike	Curve	Car_Stop	Guardrail	Color_Cone	Bump									
RGB-Thermal	CMNeXt	98.31	90.27	74.52	64.52	46.64	39.19	15.09	52.56	59.79	60.10								
RGB	Pretrained	97.79	87.62	51.13	61.94	30.05	39.36	21.04	45.55	48.95	53.71								
	Adapted	97.79	88.06	55.55	61.20	34.19	40.52	15.78	48.67	55.21	55.22								
Thermal	Pretrained	95.97	55.24	68.47	9.27	31.85	2.75	0.0	16.87	38.92	35.48								
	Adapted	97.46	82.83	70.12	49.03	40.89	26.79	1.84	36.24	52.83	50.89								

(b) Per class % IoU of pretrained and adapted CMNeXt model on MCubeS dataset.

Modalities	Methods	Asphalt	Concrete	Metal	Road_Marking	Material												Mean				
						Fabric	Glass	Plaster	Plastic	Rubber	Sand	Gravel	Ceramic	Cobblestone	Brick	Grass	Wood	Leaf	Water	Human	Sky	
RGB-A-D-N	CMNeXt	84.4	44.9	53.9	74.6	32.1	54.0	0.8	28.7	29.8	67.0	66.2	27.7	68.5	42.8	58.7	49.7	75.3	55.6	19.1	96.52	51.5
RGB	Pretrained	69.7	39.2	47.6	67.3	26.9	44.6	0.2	20.9	15.2	61.8	36.7	19.1	67.2	36.0	49.5	36.1	71.6	36.1	14.7	86.3	42.3
	Adapted	85.8	43.7	52.6	73.8	27.9	51.0	0.8	24.2	30.4	67.8	72.9	27.1	68.1	42.9	57.6	49.0	74.9	43.4	18.3	96.5	50.4
RGB-A	Pretrained	83.2	43.3	50.7	72.6	26.4	51.9	0.2	28.1	22.2	67.7	63.4	22.7	67.5	40.6	54.4	44.9	73.9	44.8	21.8	96.0	48.8
	Adapted	84.4	45.4	53.8	74.5	30.4	53.2	0.6	26.9	28.8	69.0	69.3	24.8	67.5	43.2	58.4	48.2	75.1	48.1	14.4	96.4	50.6
RGB-A-D	Pretrained	84.5	41.2	46.7	72.8	25.2	51.6	0.3	26.1	28.8	66.7	65.6	26.0	66.5	40.4	50.0	45.1	72.7	49.4	25.6	96.3	49.1
	Adapted	84.1	45.6	54.1	74.6	30.5	54.2	0.6	28.1	30.1	69.0	67.6	25.9	67.8	43.8	58.0	49.1	75.0	53.7	13.7	96.5	51.1

in mIoU, +22.05% in F1 score and +23.99% in mean accuracy over the pretrained model on an average and consistently outperforms dedicated training.

4.3 Performance Comparison for Multimodal Material Segmentation on MCubeS Dataset

We show comparison with parameter efficient model adaptation techniques on MCubeS dataset in Table 10. Scale and shift outperforms all other methods in most of the matrices for all input combinations. It also shows an improvement of +3.99% in mIoU, +3.57% in F1 score and +3.74% in mean accuracy on an average over the pretrained model. Furthermore, Scale and shift also outperforms dedicated training for all input modality combinations. These experiments corroborate the fact that scale and shift provides better model adaption for different missing modality scenarios.

5 Per Class IoU Comparison

To further analyze how the adaption is helping the model improve overall semantic and material segmentation performance, we conduct a per-class % intersection over union (IoU) analysis on the pretrained and adapted models. Table 11a and 11b summarize the results. We show the per class % IoU comparison for different missing modality situations on MFNet dataset on Table 11a. From the table we can see that when RGB is available and thermal is missing, the adaptation helps improve performance for most of the classes. Though we see some performance drop for bike (-0.74%) and guardrail (-5.25%) classes, the rest of the classes have better % IoU than the pretrained model. Bump (+6.26%), person (+4.42%), and curve (+4.14%) classes show greater improvement after adaptation. When thermal is available and RGB is missing, adaptation improves performance for all the classes. Among the classes, bike (+39.76%), car (+27.59%), car stop (+24.04%), color cone (+19.37%) and bump (+13.91%) are showing impressive performance improvement over the pretrained model.

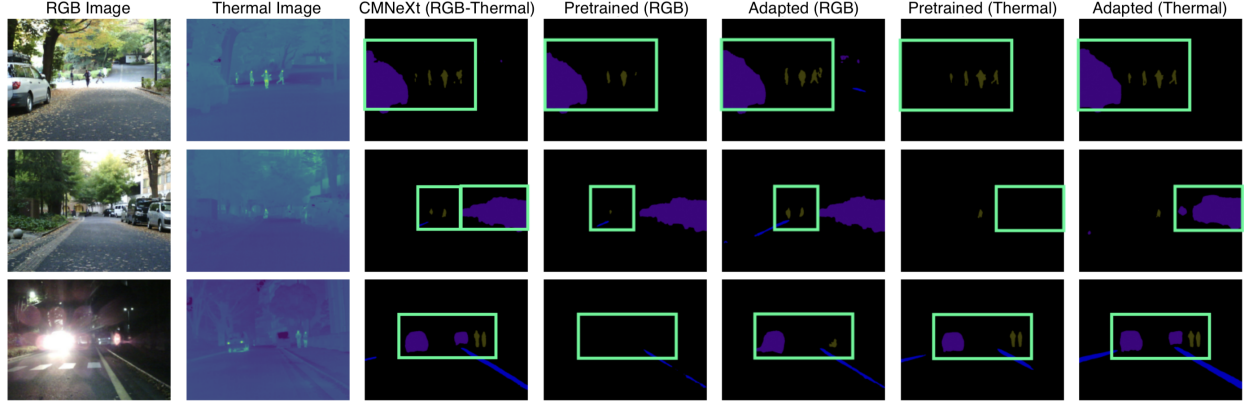
Results for MCubeS dataset is shown on Table 11b. Here A, D, and N stand for angle of linear polarization (AoLP), degree of linear polarization (DoLP) and near-infrared (NIR) respectively. Experiments show that when only RGB is available and the rest of the modalities are missing, the adapted model performs better in detecting all the 20 classes present in the dataset. Gravel (36.2%), asphalt (16.1%), rubber (15.2%), wood (12.9%) and sky (10.2%) are some of the classes who show the most performance boost after adaptation. In other input combinations, most of the classes see performance improvement compared to the pretrained model. Though we see some performance drop in a few classes, most of the classes show improvement in % IoU which leads to the overall performance improvement after adaption.

6 Visualization of Predicted Segmentation Maps

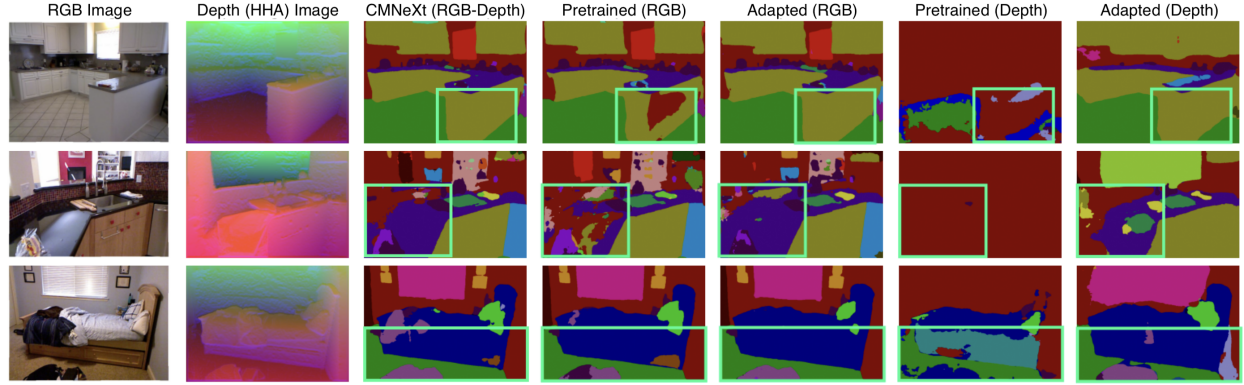
We show the predicted segmentation maps from the pretrained and adapted models in Figure 3. For each dataset, we show the input images, predictions from the base CMNeXt model when all the modalities are available, predictions from the adapted and pretrained models for different missing modality scenarios. For brevity, we only show RGB input images for MCubeS dataset. A, D and N stand for angle of linear polarization (AoLP), degree of linear polarization (DoLP) and near-infrared (NIR) respectively. Modalities that are available during testing are shown in parenthesis while other modalities are missing.

For MFNet dataset, Figure 3a shows that when only RGB is available, the pretrained model performs very poorly in detecting humans. On the other hand, if only thermal is available, the pretrained model can not detect cars very accurately. But the adapted model can detect both humans and cars more accurately in both of the scenarios. In all the cases, the predictions from the adapted model is closer to the predictions of the base CMNeXt model when all the modalities are available.

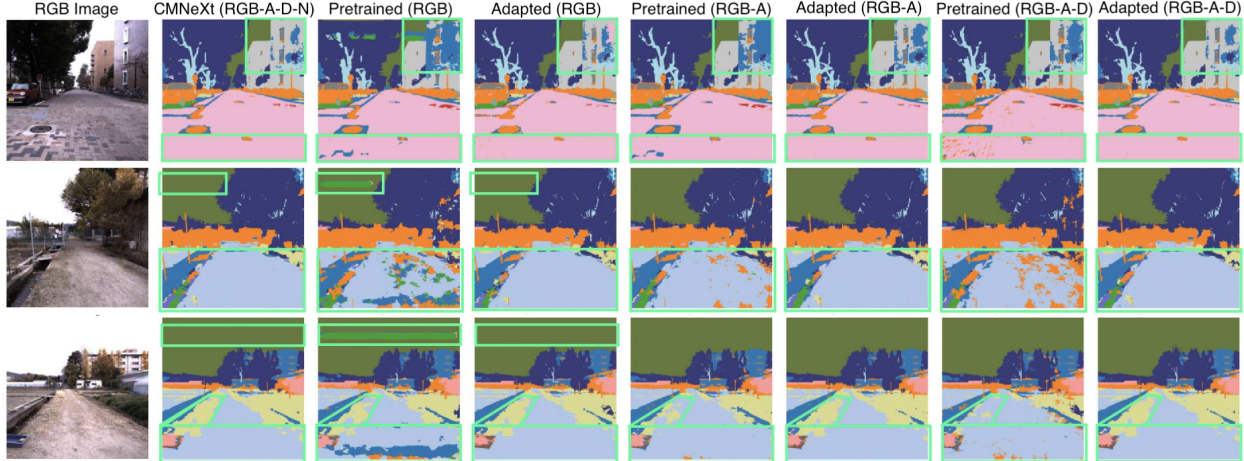
Predictions from NYUDv2 dataset is shown on Figure 3b. We can see that the adapted model can identify bed, furniture and other classes more accurately than the pretrained model for different missing modality scenarios. The pretrained model performs very poorly when only depth is available and RGB is missing. But detection accuracy improves significantly after model adaptation. For MCubeS dataset, as seen in Figure 3c, predictions from the pretrained model shows artifacts when detecting different materials. On the other hand, the adapted model is showing more accuracy in detecting sky, cobblestone, sand and brick. For all the three datasets, the predictions from the adapted model is more accurate and closer to the all modality predictions of the base CMNeXt model.



(a) Visualization of predictions on MFNet dataset



(b) Visualization of predictions on NYUDv2 dataset



(c) Visualization of predictions on MCubeS dataset

Figure 3: Visualization of predicted segmentation maps for pretrained and adapted models on MFNet and NYUDv2 datasets for multimodal semantic segmentation and MCubeS dataset for multimodal material segmentation. Only RGB images are shown from MCubeS dataset for brevity. CMNeXt column shows the predictions when all the modalities are available. Segmentation quality improves significantly after model adaptation for all the input modality combinations. A, D and N stand for angle of linear polarization, degree of linear polarization and near-infrared respectively.